

Transformations of Triphenylgermyl Ligands in Iridium–Ruthenium Carbonyl Cluster Complexes

Richard D. Adams,* Yuwei Kan, and Qiang Zhang

Department of Chemistry and Biochemistry, University of South Carolina, Columbia, South Carolina 29208, United States

Received October 15, 2010

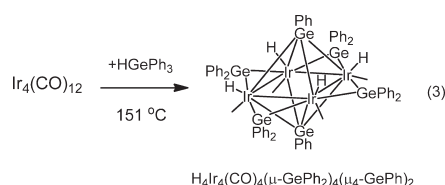
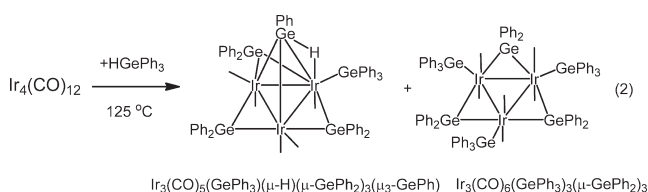
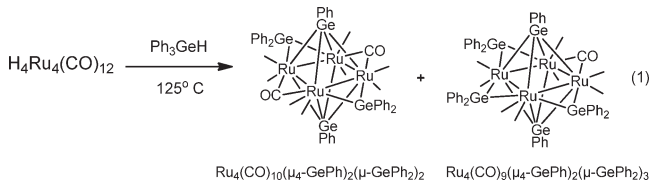
The new compound $\text{IrRu}_3(\text{CO})_{11}(\text{GePh}_3)_3(\mu\text{-H})_4$, **1**, was obtained in 64% yield from the reaction of $\text{IrRu}_3(\text{CO})_{13}(\mu\text{-H})$ with HGePh_3 at room temperature. Compound **1** has a butterfly structure for the four metal atoms with three GePh_3 ligands and four bridging hydride ligands around the periphery of the cluster. When the reaction was performed at hexane reflux for 10 min, a second, minor compound, $\text{Ir}_2\text{Ru}_2(\text{CO})_{11}(\text{GePh}_3)(\mu\text{-H})_3$, **2**, was formed. Compound **2** contains a closed cluster having two iridium and two ruthenium atoms, one GePh_3 ligand, and three bridging hydride ligands. When compound **1** was heated to 68 °C for 6 h, two new compounds, $\text{IrRu}_3(\text{CO})_{10}(\mu\text{-}\eta^2\text{-C}_6\text{H}_5)(\mu_4\text{-GePh})_2$, **3**, and $\text{IrRu}_3(\text{CO})_9(\mu\text{-}\eta^2\text{-C}_6\text{H}_5)(\mu_4\text{-GePh})_2(\mu\text{-GePh}_2)$, **4**, were formed by cleavage of phenyl rings from the GePh_3 ligands. Compounds **3** and **4** contain square IrRu_3 clusters of the metal atoms with quadruply bridging GePh germylyne ligands on opposite sides of the cluster. Both compounds also contain a rare η^5 -bridging phenyl ligand. Compound **4** was found to react with dimethylacetylenedicarboxylate (DMAD) to yield the new compound $\text{IrRu}_3(\text{CO})_9[(\mu_4\text{-Ge(Ph)C(CO}_2\text{Me)C(CO}_2\text{Me)})](\mu\text{-GePh}_2)_2$, **5**, by addition of DMAD to one of the bridging germylyne ligands. In the process the bridging phenyl ligand was transferred to the other bridging germylyne ligand to form a bridging germylene ligand.

Introduction

The coordination chemistry of germylenes has attracted considerable interest in recent years.¹ Power has synthesized the first examples of mononuclear organometallic complexes containing germylyne ligands by using sterically encumbered aryl substituents.² Germanium has been shown to be a modifier of important heterogeneous catalysts.^{3,4} Mixed metal carbonyl cluster complexes are known to be precursors to superior bi- and multimetallic heterogeneous catalysts.⁵ Accordingly, we

have been investigating the synthesis and structures of polynuclear metal carbonyl complexes containing organogerma-nium ligands for possible use as new heterogeneous catalysts.⁵

We have recently shown that HGePh_3 reacts with polynuclear ruthenium and iridium carbonyl complexes by cleavage of phenyl groups from the germanium atoms to yield complexes containing edge-bridging germylene ligands and triply bridging and quadruply bridging germylyne ligands, eqs 1–3.^{6,7}



We have now investigated the reaction of the mixed-metal iridium–ruthenium complex $\text{IrRu}_3(\text{CO})_{13}(\mu\text{-H})$ ⁸ with HGePh_3 .

*To whom correspondence should be addressed. E-mail: Adams@mail.chem.sc.edu.

(1) (a) Takaoka, M.; Mendiata, A.; Peters, J. C. *Organometallics* **2009**, 28, 3744–3753. (b) Feldman, J. D.; Peters, J. C.; Tilley, T. D. *Organometallics* **2002**, 21, 4065–4075. (c) Litz, K. E.; Banaszak Holl, M. M.; Kampf, J. W.; Carpenter, G. B. *Inorg. Chem.* **1998**, 37, 6461–6469. (d) Tokitoh, N.; Manmaru, K.; Okazaki, R. *Organometallics* **1999**, 18, 167–171.

(2) Pu, L.; Twamley, B.; Haubrich, S. T.; Olmstead, M. M.; Mork, B. V.; Simons, R. S.; Power, P. P. *J. Am. Chem. Soc.* **2000**, 122, 650–656.

(3) (a) Macleod, N.; Fryer, J. R.; Stirling, D.; Webb, G. *Catal. Today* **1998**, 46, 37–54. (b) Ponc, V. Bond, G. C. In *Catalysis by Metals and Alloys, Studies in Surface Science and Catalysis*; Elsevier: Amsterdam, 1998; Vol. 95, Chapter 13. (c) Tiong Sie, S. In *Catalytic Naphtha Reforming*; Antos, G. J.; Aitani, A. M.; Parera, J. M., Eds.; Science and Technology, Marcel Dekker Inc.: New York, 1995; Chapter 6.

(4) (a) Ekou, T.; Vicente, A.; Lafaye, G.; Especel, C.; Marecot, P. *Appl. Catal. A: Gen.* **2006**, 314, 73–80. (b) Lafaye, G.; Micaud-Especel, C.; Montassier, C.; Marecot, P. *Appl. Catal. A: Gen.* **2002**, 230, 19–30. (c) Lafaye, G.; Micaud-Especel, C.; Montassier, C.; Marecot, P. *Appl. Catal. A: Gen.* **2004**, 257, 107–117.

(5) (a) Adams, R. D.; Trufan, E. *Phil. Trans. R. Soc. A* **2010**, 368, 1473–1493. (b) Thomas, J. M.; Johnson, B. F. G.; Raja, R.; Sankar, G.; Midgley, P. A. *Acc. Chem. Res.* **2003**, 36, 20. (c) Braunstein, P.; Rose, J. In *Catalysis by Di- and Polynuclear Metal Cluster Complexes*; Adams, R. D.; Cotton, F. A., Eds.; Wiley-VCH: New York, 1998; Chapter 13. (d) Braunstein, P.; Rose, J. *Metal Clusters in Chemistry*; Braunstein, P.; Oro, L. A.; Raithby, P. R., Eds.; Wiley-VCH: Weinheim, 1999; Vol. 2, Chapter 2.2, pp 616–677.

We have observed facile oxidative-addition of HGePh_3 to the $\text{IrRu}_3(\text{CO})_{13}(\mu\text{-H})$ that leads to an opening of the cluster. Further treatment leads to cleavage of phenyl rings from the GePh_3 ligands with formation of bridging germylene and germylyne ligands. Interestingly, a phenyl ring was also observed as a bridging ligand in two of the new IrRu_3 complexes. Upon treatment with dimethylacetylenedicarboxylate, the phenyl ring of one of these complexes was shifted back from the metal atoms to a germylyne ligand. The results of these studies are reported herein.

Experimental Section

General Data. Reagent-grade solvents were dried by the standard procedures and were freshly distilled prior to use. Infrared spectra were recorded on a Thermo Nicolet Avatar 360 FT-IR spectrophotometer. ^1H NMR spectra were recorded on a Varian Mercury 300 spectrometer operating at 300.1 MHz. Mass spectrometric (MS) measurements were performed on a VG 70S instrument by using either a direct-exposure probe electron impact ionization (EI) or electrospray techniques (ES). $\text{Ru}_3(\text{CO})_{12}$ and $\text{Ir}_4(\text{CO})_{12}$ were purchased from Strem. HGePh_3 and dimethylacetylenedicarboxylate (DMAD) were purchased from Aldrich and were used without further purification. $\text{IrRu}_3(\text{CO})_{13}(\mu\text{-H})$ was prepared according to a previously reported procedure.⁸ Product separations were performed by TLC in air on Analtech 0.25 and 0.5 mm silica gel 60 Å F_{254} glass plates.

Reaction of $\text{IrRu}_3(\text{CO})_{13}(\mu\text{-H})$ with HGePh_3 . A 20.4 mg (0.0237 mmol) amount of $\text{IrRu}_3(\text{CO})_{13}(\mu\text{-H})$ was dissolved in 30 mL of hexane in a 100 mL three-neck flask. To this solution was added 30.4 mg (0.1000 mmol) of HGePh_3 , and the mixture was stirred for 8 h at room temperature. The color of the solution changed from red to dark green. The solvent was then removed *in vacuo*, and the products were separated by TLC using a 6:1 hexane/methylene chloride solvent mixture to yield 26.0 mg of dark green $\text{IrRu}_3(\text{CO})_{11}(\text{GePh}_3)_3(\mu\text{-H})_4$, **1** (64% yield). Spectral data for **1**: IR ν_{CO} (cm^{-1} in methylene chloride): 2118(vw), 2098(m), 2074(m), 2046(vs), 2030(w), 2017(m), 1998(vw). ^1H NMR (CD_2Cl_2 , in ppm) at 25 °C: δ 7.30–7.55 (m, 45H, Ph), –12.33 (s, hydride), –15.68 (s, hydride). Negative ion ES/MS: m/z 1719, $[\text{M} - \text{H}]^-$; 1691, $[\text{M} - \text{H} - \text{CO}]^-$; 1388, $[\text{M}^- - \text{CO} - \text{GePh}_3]$.

Preparation of $\text{Ir}_2\text{Ru}_2(\text{CO})_{11}(\text{GePh}_3)(\mu\text{-H})_3$, **2.** A 20.4 mg (0.0237 mmol) amount of $\text{IrRu}_3(\text{CO})_{13}(\mu\text{-H})$ was dissolved in 30 mL of hexane in a 100 mL three-neck flask. To this solution was added 30.4 mg (0.100 mmol) of HGePh_3 , and the mixture was heated to reflux for 10 min. The color of the solution changed from red to dark green. After cooling, the solvent was then removed *in vacuo*, and the products were separated by TLC using a 6:1 hexane/methylene chloride solvent mixture to yield in order of elution 0.9 mg of yellow $\text{Ir}_2\text{Ru}_2(\text{CO})_{11}(\text{GePh}_3)(\mu\text{-H})_3$, **2** (3% yield), and 4.7 mg of **1** (12% yield). Spectral data for **2**: IR ν_{CO} (cm^{-1} in methylene chloride): 2106(m), 2082(vs), 2071(s), 2057(m), 2047(m), 2028(m). ^1H NMR (CD_2Cl_2 , in ppm) at 25 °C: δ 7.32–7.51 (m, 15H, Ph), –17.81 (s, 1H, hydride), –18.79 (s, 2H, hydride). EI/MS: m/z 1202, M^+ .

Thermal Transformations of **1.** An 11.2 mg (0.0065 mmol) amount of **1** was dissolved in 30 mL of hexane in a 100 mL three-neck flask. The solution was heated to reflux for 6 h. After cooling, the solvent was removed *in vacuo*, and the products were then separated by TLC using a 6:1 hexane/methylene chloride solvent mixture to yield in order of elution 1.06 mg of green $\text{IrRu}_3(\text{CO})_{10}(\mu\text{-}\eta^2\text{-C}_6\text{H}_5)(\mu_4\text{-GePh})_2$, **3** (16.0% yield), and 2.85 mg of dark green $\text{IrRu}_3(\text{CO})_9(\mu\text{-}\eta^2\text{-C}_6\text{H}_5)(\mu_4\text{-GePh})_2$

($\mu\text{-GePh}_2$), **4** (32.4% yield). Spectral data for **3**: IR ν_{CO} (cm^{-1} in hexane): 2083(vw), 2072(m), 2056(w), 2047(vs), 2036(m), 2013(m), 2005(m), 1986(w), 1974(w). EI/MS: m/z 1153, M^+ . Spectral data for **4**: IR ν_{CO} (cm^{-1} in hexane): 2059(s), 2032(vs), 2028(vs), 2011(w), 2002(s), 1987(w), 1977(vw), 1973(vw). EI/MS: m/z 1352, M^+ .

Reaction of **4 with DMAD.** An 11.0 mg (0.0081 mmol) amount of **4** was dissolved in 30 mL of heptane in a 100 mL three-neck flask. To this solution was added 0.01 mL (0.0813 mmol) of DMAD via syringe, and the mixture was heated to reflux for 30 min. The color was changed from dark green to yellow. After cooling, the solvent was then removed *in vacuo*, and the products were separated by TLC using a 4:1 hexane/methylene chloride solvent mixture to yield 1.02 mg of yellow $\text{IrRu}_3(\text{CO})_9[(\mu_4\text{-GePh})\text{C}(\text{CO}_2\text{CH}_3)\text{C}(\text{CO}_2\text{CH}_3)](\mu\text{-GePh}_2)_2$, **5** (8.4% yield). Spectral data for **5**: IR ν_{CO} (cm^{-1} in methylene chloride): 2076(m), 2050(vs), 2023(vs), 2014(vs), 1985(m), 1966(m). ^1H NMR (CD_2Cl_2 , in ppm) at 25 °C: δ 7.36–7.78 (m, 25H, Ph), 3.77 (s, methyl), 3.61 (s, methyl). EI/MS: m/z 1466, $\text{M} - \text{CO}$.

Crystallographic Analyses. Dark green single crystals of **1** and orange single crystals of **2** suitable for X-ray diffraction analyses were obtained by slow evaporation of solvent from a hexane solvent at room temperature. Black-green single crystals of **3** and **4** and orange single crystals of **5** suitable for X-ray diffraction analyses were obtained by slow evaporation of solvent from a hexane/methylene chloride solvent mixture at –30 °C. Each data crystal was glued onto the end of a thin glass fiber. X-ray diffraction intensity data were measured by using a Bruker SMART APEX CCD-based diffractometer using Mo K α radiation ($\lambda = 0.71073$ Å). The raw data frames were integrated with the SAINT+ program by using a narrow-frame integration algorithm.⁹ Corrections for Lorentz and polarization effects were also applied with SAINT+. An empirical absorption correction based on multiple measurements of equivalent reflections was applied by using the program SADABS.⁹ All structures were solved by a combination of direct methods and difference Fourier syntheses and refined by full-matrix least-squares on F^2 by using the SHELXTL software package.¹⁰ All non-hydrogen atoms were refined with anisotropic thermal parameters. Hydrogen atoms on the phenyl rings were placed in geometrically idealized positions and included as standard riding atoms during the least-squares refinements. Compound **1** crystallized in the monoclinic system. The space groups $P2_1/n$ and Pn were indicated by the systematic absences in the data. A partial solution in the space group $P2_1/n$ that required the imposition of disorder could not be refined. This solution was thus discarded. A similar structural model obtained in the space group Pn was adequately refined as a 69/31 inversion twin without disorder. The pairs of carbonyl ligands C2–O2 and C3–O3 on Ir; C21–O21 and C22–O22 on Ru(2); C(13)–O(13) on Ru1 and C(31)–O(31) on Ru3; C33–O33 on Ru(3) and C(12)–O(12) on Ru(1); and C32–O32 on Ru3 and C11–O11 on Ru1 are related by a 2-fold pseudosymmetry. The carbon atoms of these CO ligands were restrained as these pairs in the final refinement to keep their M–C bond distances in that pair the same. The hydride ligands were located and refined by using geometric restraints (i.e., fixed Ir–H, Ru–H bond distances of 1.75 Å) and isotropic thermal parameters. Compound **2** crystallized in the triclinic crystal system. The space group $P\bar{1}$ was assumed and confirmed by the successful solution and refinement for the structure. Each hydride ligand was located and refined by using geometric restraints (i.e., fixed coordinates) and an isotropic thermal parameter. Compound **3** crystallized in the monoclinic crystal system. The systematic absences in the intensity data indicate the unique space group $P2_1/n$.

(6) Adams, R. D.; Boswell, E. M.; Captain, B.; Patel, M. A. *Inorg. Chem.* **2007**, *46*, 533–540.

(7) Adams, R. D.; Captain, B.; Smith, J. L., Jr. *Inorg. Chem.* **2005**, *44*, 1413–1420.

(8) Suss-Fink, G.; Haak, S.; Ferrand, G.; Stoeckli-Evans, H. *Dalton Trans.* **1997**, 3861–3865.

(9) SAINT+, version 6.2a; Bruker Analytical X-ray Systems, Inc.: Madison, WI, 2001.

(10) Sheldrick, G. M. *SHELXTL*, version 6.1; Bruker Analytical X-ray Systems, Inc.: Madison, WI, 1997.

Compounds **4** and **5** both crystallized in the triclinic crystal system. The centrosymmetric space group $P\bar{1}$ was selected and confirmed by the successful solution and refinement of the structure. The iridium atom Ir(1) and the ruthenium atom Ru(1) in compound **5** were disordered. These two atoms were refined by using EXYZ and EADP constraints, and the occupancies refined to nearly equal values of 0.529/0.471 on each site. Two molecules of methylene chloride from the crystallization solvent cocrystallized in the lattice with **5**. They were added to the structure factor calculation and were suitably refined by using anisotropic parameters.

Results and Discussion

The new compound $\text{IrRu}_3(\text{CO})_{11}(\text{GePh}_3)_3(\mu\text{-H})_4$, **1**, was obtained in 64% yield from the reaction of $\text{IrRu}_3(\text{CO})_{13}(\mu\text{-H})$ with HGePh_3 in hexane solvent at room temperature over a period of 8 h. Compound **1** was characterized by a combination of IR, ^1H NMR, and single-crystal X-ray diffraction analyses. An ORTEP diagram of the molecular structure of **1** is shown in Figure 1. Compound **1** consists of a butterfly cluster of one iridium and three ruthenium atoms. Atoms Ir(1) and Ru(2) occupy the "hinge" sites of the cluster, and Ru(1) and Ru(3) occupy the "wingtips" sites. The cluster is nearly planar; the dihedral angle between the planes Ru(1)–Ru(2)–Ir(1) and Ru(2)–Ru(3)–Ir(1) is 179° . The molecule contains three terminal GePh_3 ligands. Two of the GePh_3 ligands are coordinated to ruthenium atoms Ru(1) and Ru(3) and lie approximately trans to the Ir–Ru bond. The Ru–Ge distances in **1** (Ru(1)–Ge(2) = 2.5430(9) Å, Ru(3)–Ge(3) = 2.5431(9) Å) are similar to those found in the complexes $\text{Ru}_2(\text{CO})_8(\text{GePh}_3)_2$ ¹¹ (Ru(1)–Ge(1) = 2.5457(6) Å, Ru(2)–Ge(2) = 2.5413(6) Å) and $\text{Ru}_3(\text{CO})_9(\text{GePh}_3)_3(\mu\text{-H})_3$ ¹¹ (Ru–Ge = 2.5491(6), 2.5433(6), 2.5352(16) Å). The third GePh_3 ligand is coordinated to the iridium atom. The Ir–Ge distance (Ir(1)–Ge(1) = 2.5130(7) Å) is slightly shorter than the Ir–Ge distances found to the terminal GePh_3 ligands in the triiridium complex $\text{Ir}_3(\text{CO})_6(\text{GePh}_3)_3(\mu\text{-GePh}_2)_3$ ⁷ (2.5754(7), 2.5959(7), and 2.5534(8) Å).⁷ Compound **1** contains four bridging hydride ligands, one on each metal–metal bond around the periphery of the cluster. The hydride-bridged metal–metal bond distances (Ir(1)–Ru(1) = 2.9932(6) Å, Ir(1)–Ru(3) = 3.0041(6) Å, Ru(1)–Ru(2) = 3.0305(9) Å, Ru(2)–Ru(3) = 3.0316(9) Å) are significantly longer than the hinge bond (Ir(1)–Ru(2) = 2.8625(5) Å), which has no bridging ligand. Bridging hydride ligands are well known to cause lengthening to the associated metal–metal bonds.¹² The metal–metal bond distances in **1** are slightly shorter than the corresponding metal–metal bond distances in the compound $\text{IrRu}_3(\text{CO})_{11}(\text{SnPh}_3)_3(\mu\text{-H})_4$, which is the SnPh_3 homologue of **1**.¹³ All of the hydride ligands were located in the structure analysis. They exist as two inequivalent pairs in the molecule and appear as two high-field resonances of equal intensity in the ^1H NMR spectrum, $\delta = -12.33$ and -15.68 .

When solutions of $\text{IrRu}_3(\text{CO})_{13}(\mu\text{-H})$ with HGePh_3 in hexane solvent were heated to reflux for 1 h, compound **1** (12% yield) together with a small amount of the new compound $\text{Ir}_2\text{Ru}_2(\text{CO})_{11}(\text{GePh}_3)(\mu\text{-H})_3$, **2**, in 3% yield were formed. Compound **2** was characterized by a combination of

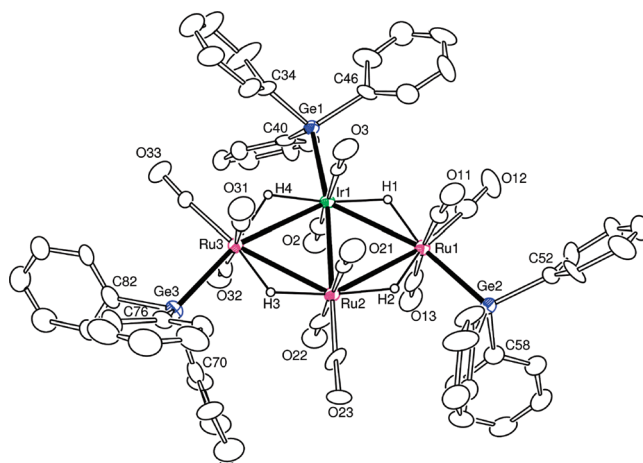


Figure 1. ORTEP diagram of $\text{IrRu}_3(\text{CO})_{11}(\text{GePh}_3)_3(\mu\text{-H})_4$, **1**, showing 30% probability thermal ellipsoids. The hydrogen atoms are omitted for clarity. Selected bond distances (in Å) are as follows: Ir(1)–Ru(1) = 2.9932(6), Ir(1)–Ru(2) = 2.8625(5), Ir(1)–Ru(3) = 3.0041(6), Ru(1)–Ru(2) = 3.0305(9), Ru(2)–Ru(3) = 3.0316(9), Ir(1)–Ge(1) = 2.5130(7), Ru(1)–Ge(2) = 2.5430(9), Ru(3)–Ge(3) = 2.5431(9).

IR, ^1H NMR, and single-crystal X-ray diffraction analyses. An ORTEP diagram of the molecular structure of **2** is shown in Figure 2. Compound **2** contains a cluster of four metal atoms: two of iridium and two of ruthenium. The cluster of **2** is closed. There are six metal–metal bonds: Ru(1)–Ru(2) = 2.8928(15) Å, Ru(1)–Ir(1) = 2.8923(12) Å, Ru(1)–Ir(2) = 2.7514(13) Å, Ir(1)–Ru(2) = 2.9007(12) Å, Ir(1)–Ir(2) = 2.7506(8) Å, Ru(2)–Ir(2) = 2.7429(13) Å. Compound **2** contains one GePh_3 ligand that is coordinated to the iridium atom Ir(1). The Ir(1)–Ge(1) = 2.5149(15) Å distance is the same as that found in **1** within experimental error. Compound **2** contains three bridging hydride ligands: one on each of the Ir–Ru bonds Ru(1)–Ir(1) and Ir(1)–Ru(2) and one on the Ir(1)–Ir(2) bond. As expected, the hydride-bridged metal–metal bonds are significantly longer than the unbridged bonds.¹² The ^1H NMR spectrum exhibits two high-field resonances, $\delta = -17.81$ (s, 1H), -18.79 (s, 2H), that are assigned to the three hydride ligands. There are 11 linear terminal carbonyl ligands distributed among the metal atoms as shown in Figure 2. Overall, the cluster contains a total of 60 valence electrons, which is exactly the number required for a tetrahedral cluster complex in which each of the metal atoms obeys the 18-electron rule. Compound **2** is remarkably similar to its tin homologue $\text{Ir}_2\text{Ru}_2(\text{CO})_{11}(\text{SnPh}_3)(\mu\text{-H})_3$, which was recently obtained from the reaction of $\text{IrRu}_3(\text{CO})_{13}(\mu\text{-H})$ with HSnPh_3 .¹³

Two new compounds, $\text{IrRu}_3(\text{CO})_{10}(\mu\text{-}\eta^2\text{-C}_6\text{H}_5)(\mu_4\text{-GePh})_2$, **3** (16 yield), and $\text{IrRu}_3(\text{CO})_9(\mu\text{-}\eta^2\text{-C}_6\text{H}_5)(\mu_4\text{-GePh})_2(\mu\text{-GePh}_2)$, **4** (32% yield), were obtained when a solution of **1** in hexane solvent was heated to reflux (68°C) for 6 h. Both compounds were characterized by a combination of IR, ^1H NMR, MS, and single-crystal X-ray diffraction analyses. An ORTEP diagram of the molecular structure of **3** is shown in Figure 3. Compound **3** contains a planar cluster of four metal atoms, one of iridium and three of ruthenium. There are two quadruply bridging phenylgermylidyne ligands on opposite sides of the cluster that were formed by cleavage of phenyl groups from the GePh_3 ligands in **1**. The Ru–Ru bond distances are significantly different: Ru(1)–Ru(3) = 2.9823(6) Å, while Ru(2)–Ru(3) is 2.8690(6) Å. The difference in lengths may be related to steric

(11) Adams, R. D.; Captain, B.; Trufan, E. *J. Cluster Sci.* **2007**, *18*, 642–659.

(12) (a) Bau, R.; Drabnis, M. H. *Inorg. Chim. Acta* **1997**, *259*, 27–50. (b) Teller, R. G.; Bau, R. *Struct. Bonding* **1981**, *41*, 1–82.

(13) Adams, R. D.; Kan, Y.; Trufan, E.; Zhang, Q. *J. Cluster Sci.* **2010**, *21*, 371–378.

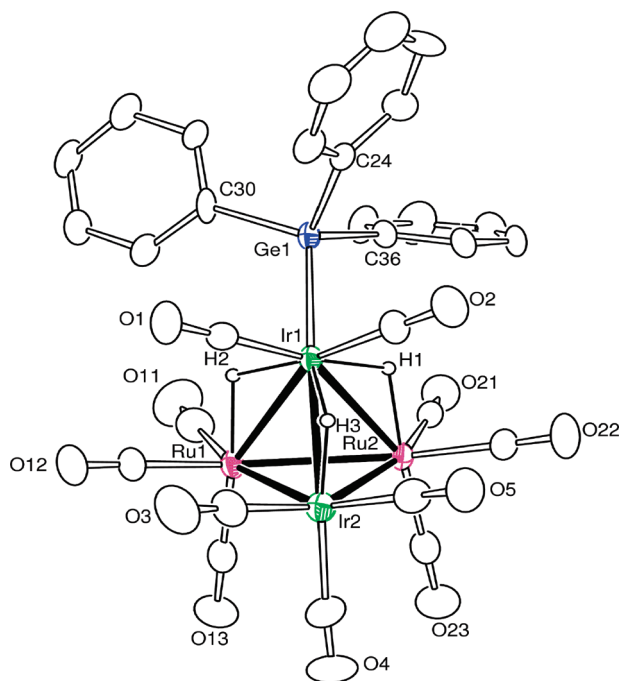


Figure 2. ORTEP diagram of $\text{Ir}_2\text{Ru}_2(\text{CO})_{11}(\text{GePh}_3)(\mu\text{-H})_3$, **2**, showing 30% probability thermal ellipsoids. The hydrogen atoms are omitted for clarity. Selected interatomic bond distances (in Å) are as follows: Ir(1)–Ge(1) = 2.5149(15), Ru(1)–Ru(2) = 2.8928(15), Ru(1)–Ir(1) = 2.8923(12), Ru(1)–Ir(2) = 2.7514(13), Ir(1)–Ru(2) = 2.9007(12), Ir(1)–Ir(2) = 2.7506(8), Ru(2)–Ir(2) = 2.7429(13).

effects; in particular, atoms Ru(1) and Ru(3) both contain three terminal carbonyl ligands, while Ru(2) has only two carbonyl ligands. The cluster complexes $\text{Ru}_4(\text{CO})_8(\mu\text{-CO})_2(\mu_4\text{-GePh})_2$ ($\mu\text{-GePh}_2$)₂, **6**, $\text{Ru}_4(\text{CO})_8(\mu\text{-CO})(\mu_4\text{-GePh})_2(\mu\text{-GePh}_2)_3$, **7**, and $\text{Ru}_4(\text{CO})_8(\mu_4\text{-GePh})_2(\mu\text{-GePh}_2)_4$, **8**, also have quadruply bridging germylyne ligands on opposite sides of a similar arrangement of four metal atoms, eq 1.⁶ The Ir–Ru bond distances also have significantly different lengths. The Ir(1)–Ru(2) bond distance of 2.6485(5) Å is nearly 0.30 Å shorter than the Ir(1)–Ru(1) distance of 2.9368(5) Å. The short length of the Ir(1)–Ru(2) bond can be attributed to the presence of a bridging phenyl ligand across that bond. The Ru–Ge bond distances span a considerable range, 2.4582(7)–2.7147(7) Å, which is probably due to sterics and asymmetrical bonding introduced by the presence of the bridging phenyl ligand across the Ir(1)–Ru(2) bond. The Ir–Ge distances are of similar lengths (Ir(1)–Ge(1) = 2.5737(6) Å, Ir(1)–Ge(2) = 2.5138(6) Å) and are slightly longer than those observed for the quadruply bridging germylyne ligands in the tetrairidium complex $\text{H}_4\text{Ir}_4(\text{CO})_4(\mu_4\text{-GePh})_2(\mu\text{-GePh}_2)_4$, 2.44–2.47 Å.⁷ Although bridging phenyl rings are not common, a number of examples have been

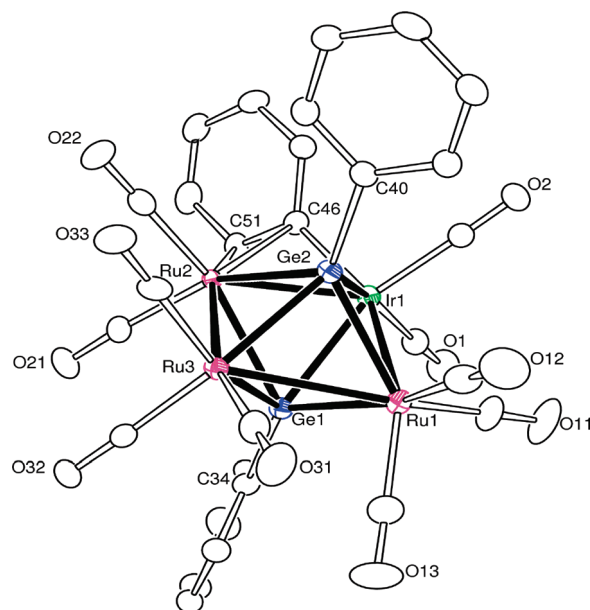


Figure 3. ORTEP diagram of $\text{IrRu}_3(\text{CO})_{10}(\mu\text{-}\eta^2\text{-C}_6\text{H}_5)(\mu_4\text{-GePh})_2$, **3**, showing 40% probability thermal ellipsoids. The hydrogen atoms are omitted for clarity. Selected bond distances (in Å) are as follows: Ir(1)–Ru(1) = 2.9368(5), Ir(1)–Ru(2) = 2.6485(5), Ir(1)–Ge(1) = 2.5737(6), Ir(1)–Ge(2) = 2.5138(6), Ru(1)–Ru(3) = 2.9823(6), Ru(1)–Ge(1) = 2.4582(7), Ru(1)–Ge(2) = 2.5253(7), Ru(2)–Ru(3) = 2.8690(6), Ru(2)–Ge(1) = 2.6035(7), Ru(2)–Ge(2) = 2.7147(7), Ru(3)–Ge(1) = 2.5422(7), Ru(3)–Ge(2) = 2.4693(7), Ir(1)–C(46) = 2.083(6), Ru(2)–C(46) = 2.260(5), Ru(2)–C(51) = 2.441(6).

structurally characterized in metal carbonyl cluster complexes and polynuclear metal coordination complexes.¹⁴

The bridging phenyl ligand observed in **3** is unusual because two of its carbon atoms, C(46) and C(51), are coordinated to the metal atoms. The ipso carbon C(46) is bonded to the two metal atoms Ir(1) and Ru(2) (Ir(1)–C(46) = 2.083(6) Å, Ru(2)–C(46) = 2.260(5) Å), while C(51) is bonded only to Ru(2) (Ru(2)–C(51) = 2.441(6) Å). There are very few examples of a $\mu\text{-}\eta^2$ -bridging phenyl ligand in the literature. These include $\text{MoRhPt}(\text{C}_5\text{H}_5)(\text{PPh}_3)_2(\mu\text{-CO})_2(\mu\text{-PPh}_2)(\mu\text{-}\eta^2\text{-C}_6\text{H}_5)$,¹⁵ $\text{Ru}_3(\text{CO})_7(\text{PPh}_3)(\mu\text{-PPh}_2)(\mu\text{-}\eta^2\text{-C}_6\text{H}_5)(\mu_3\text{-S})$,¹⁶ and $\text{RuIr}(\text{C}_5\text{Me}_5)_2(\text{PPh}_3)_2(\mu\text{-H})(\mu\text{-PPh}_2)(\mu\text{-}\eta^2\text{-C}_6\text{H}_5)$,¹⁷ all of which were formed by the cleavage of a phenyl ring from a PPh_3 ligand, and $\text{Ru}_2(\text{C}_5\text{H}_5)_2(\text{CO})_2(\text{SnMePh}_2)(\mu\text{-}\eta^2\text{-C}_6\text{H}_5)$ ¹⁸ and $\text{Mo}_2(\text{C}_5\text{H}_5)_2(\text{NO})_2[\mu\text{-P}(\text{C}_6\text{H}_{11})_2](\mu\text{-}\eta^2\text{-C}_6\text{H}_5)$.¹⁹

Compound **3** contains 10 linear terminal carbonyl ligands distributed as shown in Figure 3. The GePh ligands and the bridging phenyl ligand each serve as a three-electron donor. Each of the ruthenium atoms thus achieves an 18-electron configuration, but the iridium atom has only 16 electrons. Alternatively, a delocalized bonding model as represented by the polyhedral skeletal electron pair approach would predict a total valence electron count of 62 electrons for

(14) (a) Adams, R. D.; Pearl Jr., W. C. *J. Organomet. Chem.* **2010**, doi:10.1016/j.jorganchem.2010.08.046. (b) Adams, R. D.; Captain, B.; Zhu, L. *Organometallics* **2006**, *25*, 4183–4187. (c) Cabeza, J. A.; Franco, R. J.; Llamazares, A.; Riera, V.; Perez-Carreño, E.; Van der Maelen, J. F. *Organometallics* **1994**, *13*, 55–59. (d) Delavaux, B.; Chaudret, B.; Dahan, F.; Poilblanc, R. *Organometallics* **1985**, *4*, 935–937. (e) Harding, M. M.; Nicholls, B. S.; Smith, A. K. *J. Chem. Soc., Dalton Trans.* **1983**, 1479–1481. (f) Jans, J.; Naegeli, R.; Venanzi, L. M.; Albinati, A. *J. Organomet. Chem.* **1983**, *247*, C37–C41. (g) Taylor, N. J.; Chieh, P. C.; Carty, A. J. *J. Chem. Soc., Chem. Commun.* **1975**, 448. (h) Bradford, C. W.; Nyholm, R. S.; Gainsford, G. J.; Guss, J. M.; Ireland, P. R.; Mason, R. J. *J. Chem. Soc., Chem. Commun.* **1972**, 87–89. (i) Bradford, C. W.; Nyholm, R. S. *J. Chem. Soc., Dalton Trans.* **1973**, 529–533.

(15) Farrugia, L. J.; Miles, A. D.; Stone, F. G. A. *J. Chem. Soc., Dalton Trans.* **1984**, 2415–2422.

(16) Hoferkamp, L. A.; Rheinwald, G.; Stoeckli-Evans, H.; Suss-Fink, G. *Organometallics* **1996**, *15*, 704–712.

(17) Shima, T.; Suzuki, H. *Organometallics* **2005**, *24*, 1703–1708.

(18) Akita, M.; Hua, R.; Oku, T.; Tanaka, M.; Moro-oka, Y. *Organometallics* **1996**, *15*, 4162–4177.

(19) Alvarez, M. A.; Garcia, M. E.; Martinez, M. E.; Ramos, A.; Ruiz, M. A. *Organometallics* **2009**, *28*, 6293–6307.

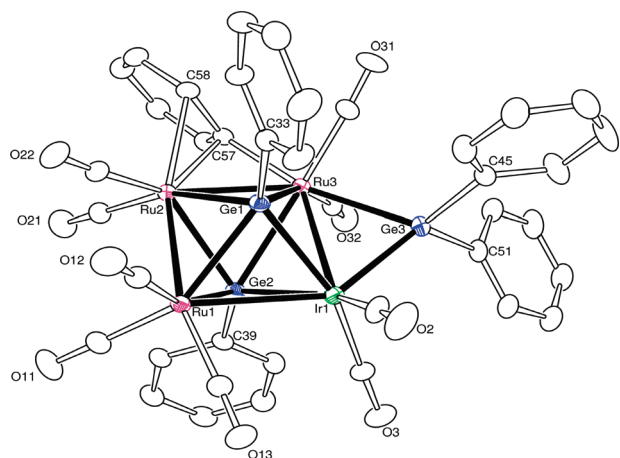


Figure 4. ORTEP diagram of $\text{IrRu}_3(\text{CO})_9(\mu\text{-}\eta^2\text{-C}_6\text{H}_5)(\mu_4\text{-GePh}_2)(\mu\text{-GePh}_2)$, **4**, showing 20% probability thermal ellipsoids. The hydrogen atoms are omitted for clarity. Selected bond distances (in Å) are as follows: Ir(1)–Ru(1) = 2.9519(3), Ir(1)–Ru(3) = 2.9188(3), Ir(1)–Ge(1) = 2.4920(4), Ir(1)–Ge(2) = 2.5228(4), Ir(1)–Ge(3) = 2.4098(4), Ru(1)–Ru(2) = 2.8932(4), Ru(1)–Ge(1) = 2.5267(4), Ru(1)–Ge(2) = 2.4943(4), Ru(2)–Ru(3) = 2.6994(4), Ru(2)–Ge(1) = 2.5956(5), Ru(2)–Ge(2) = 2.5555(4), Ru(3)–Ge(1) = 2.6203(4), Ru(3)–Ge(2) = 2.6058(4), Ru(3)–Ge(3) = 2.5822(5), Ru(2)–C(57) = 2.215(3), Ru(3)–C(57) = 2.121(3), Ru(2)–C(58) = 2.360(3).

an arachnooctahedron of four metal atoms, which is precisely the number of valence electrons found in complex **3**.²⁰

An ORTEP diagram of the molecular structure of **4** is shown in Figure 4. The structure of **4** is somewhat similar to **3**. Compound **4** contains four metal atoms, one of iridium and three of ruthenium in a square arrangement, and two quadruply bridging phenylgermylyne ligands. However, compound **4** has an edge-bridging GePh_2 ligand on one of the Ir–Ru bonds and one less terminal CO ligand. Like **3**, compound **4** also contains a $\mu\text{-}\eta^2$ -bridging phenyl ligand, but in **4** this ligand bridges a Ru–Ru bond instead of the Ir–Ru bond as found in **3**. As found in **3**, the phenyl-bridged metal–metal bond, Ru(2)–Ru(3) = 2.6994(4) Å, is considerably shorter than the unbridged Ru–Ru bond, Ru(1)–Ru(2) = 2.8932(4) Å. As with **3**, compound **4** contains a total of 62 valence electrons, which is consistent with the bonding model represented by the polyhedral skeletal electron pair approach.²⁰

In order to investigate its reactivity, a solution of compound **4** in heptane solvent was treated with $(\text{MeO}_2\text{C})\text{C}_2(\text{CO}_2\text{Me})$ (DMAD) and heated to reflux for 30 min. From this reaction mixture, the new compound $\text{IrRu}_3(\text{CO})_9[(\mu_4\text{-Ge(Ph)C(CO}_2\text{Me)C(CO}_2\text{Me)})](\mu\text{-GePh}_2)_2$, **5**, was obtained in 8.4% yield. Compound **5** was characterized by a combination of IR, ^1H NMR, MS, and single-crystal X-ray diffraction analyses. An ORTEP diagram of the molecular structure of **5** is shown in Figure 5. Compound **5** contains a butterfly cluster of four metal atoms, one of iridium and three of ruthenium. The iridium atom occupies one of the wingtip positions, and in the crystal, Ir(1) and Ru(3) in the other wingtip position are equally disordered. There are two GePh_2 ligands that bridge the adjacent hinge–wingtip bonds Ru(1)–Ir(1) and Ru(1)–Ru(3). One of these GePh_2 ligands was evidently formed by a shift of the bridging phenyl ligand in **4** to one of the bridging GePh ligands because **4** has only one GePh_2 ligand.

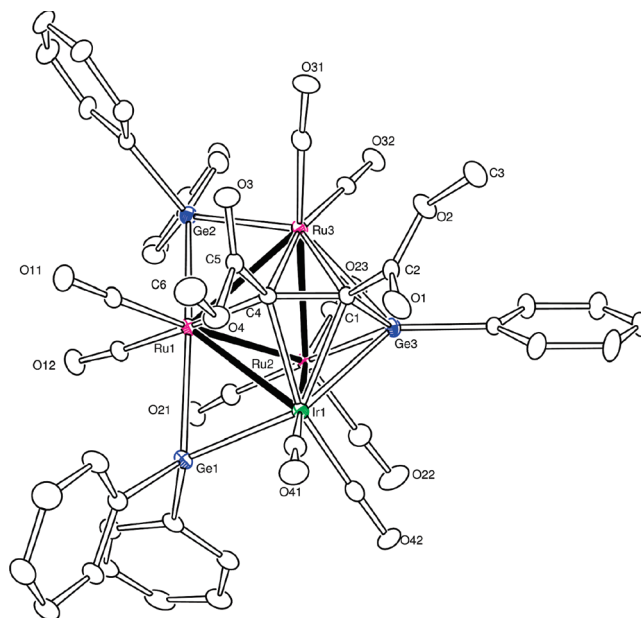


Figure 5. ORTEP diagram of $\text{IrRu}_3(\text{CO})_9(\mu\text{-GePh}_2)[\mu_4\text{-Ge(Ph)C(CO}_2\text{CH}_3)\text{C(CO}_2\text{CH}_3)]$, **5**, showing 10% probability thermal ellipsoids. The hydrogen atoms are omitted for clarity. Selected bond distances (in Å) are as follows: Ir(1)–Ru(1) = 2.8428(7), Ir(1)–Ru(2) = 2.9543(7), Ir(1)–Ge(1) = 2.4384(8), Ir(1)–Ge(3) = 2.6475(9), Ru(1)–Ru(2) = 2.9094(8), Ru(1)–Ru(3) = 2.8302(7), Ru(1)–Ge(1) = 2.5434(10), Ru(1)–Ge(2) = 2.5294(10), Ru(2)–Ru(3) = 2.9677(7), Ru(2)–Ge(3) = 2.3820(9), Ru(3)–Ge(2) = 2.4356(8), Ru(3)–Ge(3) = 2.5906(9), Ge(3)–C(1) = 1.947(6), C(1)–C(4) = 1.448(9).

One equivalent of DMAD was added to **4** in the reaction. The DMAD has formed a bond to one of the GePh ligands by using one of the alkyne carbon atoms, $\text{Ge(3)–C(1)} = 1.947(6)$ Å. The entire $(\text{CH}_3\text{O}_2\text{C})\text{C(CO}_2\text{CH}_3)\text{CGePh}$ group serves a quadruply bridging ligand across all four metal atoms, and the alkyne C–C bond, C(1)–C(4), has lengthened to 1.448(9) Å due to the coordination. This C–C distance is similar to the C–C distances found for the quadruply bridging DMAD ligands found in the complex $\text{CoRh}_3(\text{CO})_9[\mu_4\text{-(CH}_3\text{O}_2\text{C)-C}_2(\text{CO}_2\text{CH}_3)]_2[\mu_4\text{-(CH}_3\text{O}_2\text{C)C}_2(\text{CO}_2\text{CH}_3)]$, 1.411(6) and 1.428(6) Å.²¹ The formation of germanium–carbon bonds is central to reactions such as the hydrogermylation of alkynes.²² Mochida et al. has shown that digermanes can be added to alkynes catalytically in the presence of certain platinum complexes.²³

If one counts the $(\text{CH}_3\text{O}_2\text{C})\text{C(CO}_2\text{CH}_3)\text{CGePh}$ ligand as a five-electron donor, then the cluster has a total of 60 valence electrons, which is two short of the requirements for an 18-electron configuration at each metal atom in a cluster of four

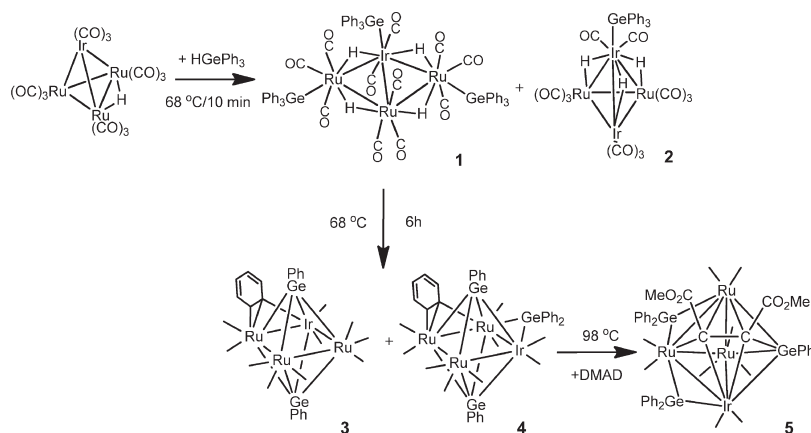
(20) Mingos, D. M. P. *Acc. Chem. Res.* **1984**, *17*, 311–319.

(21) Watson, W. H.; Poola, B.; Richmond, M. G. *Organometallics* **2005**, *24*, 4687–4690.

(22) (a) Takanori Matsuda, T.; Kadowaki, S.; Yamaguchi, Y.; Murakami, M. *Org. Lett.* **2010**, *12*, 1056–1058. (b) Corriu, R. J. P.; Moreau, J. J. E. *J. Chem. Soc., D* **1971**, 812. (c) Esteruelas, M. A.; Martin, M.; Oro, L. A. *Organometallics* **1999**, *18*, 2267–2270. (d) Kinoshita, H.; Nakamura, T.; Kakiya, H.; Shinokubo, H.; Matsubara, S.; Oshima, K. *Org. Lett.* **2001**, *3*, 2521–2524. (e) Marciniak, B.; Lawicka, H.; Majchrzak, M.; Kubicki, M.; Kownacki, I. *Chem.—Eur. J.* **2006**, *12*, 244–250. (f) David-Quillot, F.; Thierry, V.; Abarbri, M.; Thibonnet, J.; Besson, T.; Duchene, A. *Trans. Met. Chem.* **2007**, *30*, 235–244. (g) Ichinose, Y.; Oda, H.; Oshima, K.; Utimoto, K. *Bull. Chem. Soc. Jpn.* **1987**, *60*, 3468–3470.

(23) Mochida, K.; Wada, T.; Suzuki, K.; Hatanaka, W.; Nishiyama, Y.; Nanjo, M.; Sekine, A.; Ohashi, Y.; Masato Sakamoto, M.; Yamamoto, A. *Bull. Chem. Soc. Jpn.* **2001**, *74*, 123–137.

Scheme 1



metal atoms with five metal–metal bonds. Alternatively, if one views the germanium atom and carbon atoms C(1) and C(4) as part of the cluster, then the cluster could be regarded as a closo-pentagonal bipyramidal framework and the total valence electron count would be 70, which is exactly the number predicted for this delocalized bonding model by the polyhedral skeletal electron pair theory.²⁰

Summary

A summary of the reactions reported here is shown in Scheme 1. The closed cluster complex $\text{IrRu}_3(\text{CO})_{13}(\mu\text{-H})$ eliminated two equivalents of CO and was opened to form the tris- GePh_3 complex **1** in good yield by the oxidative addition of three equivalents of HGePh_3 when the reaction was performed at room temperature. Compound **1** was also formed but in a significantly lower yield together with minor coproduct **2** when the reaction was performed at 68°C . Compound **2** has a different metal composition than **1**, which is obviously the result of a complex metal–metal exchange reaction that could also account for its low yield.

When compound **1** was heated to 68°C for an extended period, the phenyl groups were cleaved from the GePh_3 ligands and the complexes **3** and **4** were formed. Both of these complexes contain two quadruply bridging germylyne

ligands positioned on opposite sides of a square cluster of four metal atoms. Compound **4** also contains an edge-bridging GePh_2 ligand. Interestingly, one of the cleaved phenyl groups was retained in each of these products in the form of a rare η^2 -bridging ligand. Even more interestingly, it was found that the bridging phenyl ligand in **4** could be passed back to one of the bridging germylyne ligands upon addition of DMAD to the complex, and the added DMAD formed a bond to the other germylyne ligand. It is hoped that these new mixed-metal germanium complexes will prove to be useful precursors to new heterogeneous catalysts for the hydrogenation of unsaturated hydrocarbons.^{3,4}

Acknowledgment. This research was supported by the National Science Foundation under Grant No. CHE-0743190. We thank the USC NanoCenter for partial support of this work. We thank Dr. Mark Smith for assistance with some of the crystal structure analyses.

Supporting Information Available: CIF tables for the structural analyses of compounds **1**–**5**. Table S1 contains crystal data, data collection parameters, and results of the analyses. This material is available free of charge via the Internet at <http://pubs.acs.org>.